Highly active heterogeneous Fenton-like systems based on Fe^0/Fe$_3$O$_4$ composites prepared by controlled reduction of iron oxides

Regina C.C. Costa [a], Flávia C.C. Moura [b], J.D. Ardisson [c], J.D. Fabris [a], R.M. Lago [a],*

[a] Departamento de Química, ICEx, Universidade Federal de Minas Gerais UFMG, 31270-901 Belo Horizonte, MG, Brazil
[b] Departamento de Química, ICEB, Universidade Federal de Ouro Preto UFOP, 35400-000 Ouro Preto, MG, Brazil
[c] Laboratório de Física Aplicada, Centro de Desenvolvimento e Tecnologia Nuclear (CDTN), 31270-901 Belo Horizonte, MG, Brazil

Abstract

In this work, a new and highly active heterogeneous Fenton system based on iron metal and magnetite Fe^0/Fe$_3$O$_4$ composites has been prepared by controlled reduction of iron oxides. Temperature-programmed reduction experiments with H$_2$ showed that iron oxides, i.e. Fe$_2$O$_3$, FeOOH and Fe$_3$O$_4$, can be reduced to produce highly reactive Fe^0/Fe$_3$O$_4$ composites with different metal to oxide ratios as determined by Mössbauer spectroscopy and powder X-ray diffraction. Mössbauer measurements revealed that these composites are reactive towards gas phase molecules and can be oxidized rapidly by O$_2$ even at room temperature. The composites showed also very high activity for the Fenton chemistry, i.e. the oxidation of an organic model contaminant, the dye methylene blue, and the H$_2$O$_2$ decomposition. The best results were obtained with the composites with 47% Fe^0 obtained by reduction of Fe$_3$O$_4$ with H$_2$ at 400 °C for 2 h, which produced a very rapid discoloration with total organic carbon (TOC) removal of 75% after 2 h reaction. Conversion electron Mössbauer spectroscopy (CEMS) measurements before and after H$_2$O$_2$ reaction showed that Fe$_3$O$_4$ and especially Fe^0 are oxidized during the reaction. The reaction mechanism is discussed in terms of the formation of HO$^•$ radicals by a Haber–Weiss initiated by an efficient electron transfer from the composite Fe^0/Fe$_3$O$_4$ to H$_2$O$_2$. The higher activity of the composites compared to the pure Fe^0 and iron oxides has been explained by two possible effects, i.e. (i) a thermodynamically favorable electron transfer from Fe^0 to Fe$_3$O$_4$ producing Fe^{2+}$_{magnetite}$ active for the reaction and (ii) by the formation of very reactive small particle size Fe^0 and Fe$_3$O$_4$.
© 2008 Elsevier B.V. All rights reserved.

Keywords: Heterogeneous Fenton; Composites; Oxidation

1. Introduction

The Fenton reagent (a mixture of Fe^{2+} and H$_2$O$_2$) is one of the most active systems for the oxidation of organics in water [1–3]. This reactivity is due to the *in situ* generation of highly oxidative species, i.e. hydroxyl radicals, according to the process:

$$Fe^{2+}_{(aq)} + H_2O_2 \rightarrow Fe^{3+}_{(aq)} + OH^- + OH^• \qquad (1)$$
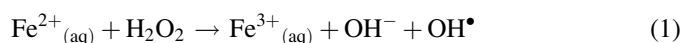
The Fenton reaction operates at the optimum pH 3 and requires stoichiometric amounts of Fe^{2+}. After the process the effluent must be neutralized generating significant amounts of sludge, which is a limitation of the process due to disposal problems [3].

The development of active heterogeneous Fenton systems, where soluble Fe^{2+} is replaced by Fe-containing solids with no need of low pH is of considerable interest. These heterogeneous Fenton systems could offer some advantages over the classical homogeneous reaction, such as no sludge formation, operation at near neutral pH and the possibility to recycle the iron promoter [4].

Several recent studies have investigated different iron solid compounds to replace the soluble Fe^{2+} in order to design new heterogeneous Fenton-like system. Some of the iron containing solids investigated were goethite, hematite, clay minerals, iron hydroxide and iron supported on silica and on alumina [5–10]. However, these iron promoters showed low activities or strong iron leaching due to low pH which produced mainly homogeneous reactions.

Hereon, we report our results on a new heterogeneous Fenton system based on Fe$_3$O$_4$ combined with Fe^0 metal. The inverse spinel magnetite, Fe$_3$O$_4$, has several important features

---

* Corresponding author. Tel.: +55 31 3409 57777; fax: +55 31 3409 5700.
E-mail address: rochel@ufmg.br (R.M. Lago).

for a Fenton reaction, e.g. (i) it contains $Fe^{2+}_{magnetite}$ which might play an important role as an electron donor to initiate the Fenton reaction according to the classical Haber–Weiss mechanism, (ii) the octahedral site in the magnetite structure can easily accommodate both Fe^{2+} and Fe^{3+}, which means that Fe^{2+} can be reversibly oxidized and reduced back in the same structure and (iii) isostructural substitution of iron by different transition metals can tune the physical–chemical properties of magnetites to produce more active systems. Despite these characteristics scarce work has been carried out with magnetite in heterogeneous Fenton systems [11–16].

Metallic iron, Fe^0, has been studied as a low cost and innocuous reductant in different environmental remediation processes, e.g. permeable reactive barriers [17] reduction of organochloro [18], dyes [19,20], pesticides [21], Cr(VI) [22] and As [23]. There are also some attempts to use Fe^0 instead Fe^{2+}_{aq} for the Fenton reaction since iron metal can potentially participate in the reaction with three electrons. Fe^0/H^+ has been proposed as a precursor of Fe^{2+} in Fenton reactions which is not advantageous since two electrons are spent to produce H_2 and Fe^{2+} [24,25]. However, in a near neutral pH media the direct electron transfer from Fe^0 to H_2O_2 in a Haber–Weiss-like mechanism during a Fenton reaction is a very slow process.

In previous work, we have demonstrated that the combination of Fe^0 and Fe_3O_4 by simply grinding the powder mixtures produces a strong increase in activity for the Fenton reaction [26–28]. The increase in activity was discussed in terms of a thermodynamically favorable electron transfer from Fe^0 to $Fe^{3+}_{magnetite}$ species. This electron transfer during the reaction can regenerate the $Fe^{2+}_{magnetite}$ which are the active species for the Fenton reaction.

In this work, composites Fe^0/Fe_3O_4 have been prepared by controlled reduction of Fe_3O_4 with H_2 and completely characterized by Mössbauer spectroscopy, powder XRD and magnetization measurements. These composites showed high activity for the Fenton chemistry offering possibilities to design new heterogeneous advanced oxidation systems for the treatment of wastewater. Also, it opens the possibility to use different iron precursors, for example wastes and natural materials containing iron oxides which can be easily reduced by different agents.

2. Experimental

The magnetite, Fe_3O_4, was prepared by coprecipitation of the precursor ferric hydroxyacetate followed by thermal treatment at 430 °C under N_2 atmosphere [29].

The composites were prepared by thermal treatment at 300 °C, 400 °C and 500 °C (heating at 10 °C min^{-1}) in a quartz tube under H_2 (99.99%) flow (30 mL min^{-1}) for 1 min up to 4 h. After reduction the material was cooled down under H_2 flow to room temperature and was transferred to a sample vial (some? exposition to air occurred in this step) and kept under nitrogen to avoid slow oxidation by air.

Mössbauer spectroscopy was used to identify and quantify the iron phases present in the samples using transmission and backscattering modes. In the transmission mode bulk analyses

can be carried out by transmitted photons. In the backscattering geometry, as in conversion electron Mössbauer spectroscopy (CEMS), Auger conversion electrons (7.3 keV) are analyzed. The CEMS analysis affords information of the more superficial layer of the material with approximately 3000 Å depth. The Mössbauer experiments were carried out in a spectrometer CMTE model MA250 with a ^{57}Co/Rh source at room temperature using α-Fe^0 as reference. The CEMS was performed at room temperature using a conventional spectrometer with a throwing gas (95% helium and 5% methane), proportional counter and a ^{57}Co. The γ-ray beam was oriented perpendicular to the sample.

Magnetization measurements were carried out in a portable magnetometer with magnetic field of 0.3 T calibrated with Ni metal [30]. The powder XRD data were obtained in a Rigaku model Geigerflex using Cu Kα radiation scanning from 2° to 75° at a scan rate of 4° min^{-1}. Lattice parameters were obtained using the program UNITCELL? and the average crystallite size estimated by the Scherrer's equation. Scanning electron microscopy (SEM) analyses were carried out in a Jeol JKA 8900RL. TPR experiments were carried out in a Quantachrome CHEMBET using H_2 5% in N_2 at a heating rate of 10 °C min^{-1}.

The hydrogen peroxide (Synth) decomposition was carried out with 7 mL solution at [H_2O_2] 2.7 mol L^{-1}, pH 5.5 ± 0.2 (natural pH of the H_2O_2 solution) with 30 mg catalyst by measuring the formation of gaseous O_2 in a simple volumetric glass system based on a burette connected to the reaction system. The reaction system was magnetically stirred in a recirculating temperature-controlled bath kept at 25 ± 1 °C. The oxidation of the dye methylene blue 10 mL at the concentration of 100 mg L^{-1} was carried out with H_2O_2 (0.3 mol L^{-1}) at pH 6.0 ± 0.2 (natural pH of the H_2O_2 solution) with 30 mg of catalyst and monitored by UV–vis measurements. All the reactions were carried out under magnetic stirring in a recirculating temperature-controlled bath kept at 25 ± 1 °C. The total organic carbon (TOC) measurements were carried out in equipment Shimadzu TOC5000.

3. Results and discussion

3.1. Preparation and characterization of the Fe^0/Fe_3O_4 composites

The composites Fe^0/Fe_3O_4 were prepared by controlled reduction of the starting Fe_3O_4 with H_2. This reduction takes place in a multi-step process as suggested by TPR analyses (Fig. 1):

The TPR profile shows a first reduction process in the temperature range 300–450 °C with a peak centered at 385 °C. As suggested by XRD and Mössbauer spectroscopic (MS) analyses (not presented) and previous work [29], the sample obtained by a TPR experiment interrupted at 400 °C and the sample quenched to room temperature, this reduction is related to the presence of small amounts of oxidized phases such as Fe_2O_3 and FeOOH which are reduced to Fe_3O_4.

$$Fe_2O_3/FeO(OH)/Fe_3O_{4+\delta} + H_2 \rightarrow Fe_3O_4 + nH_2O \qquad (2)$$
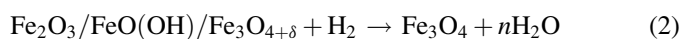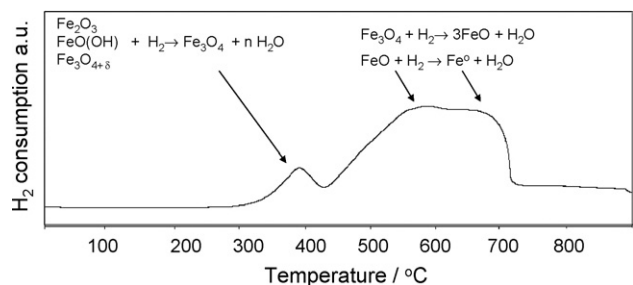
Fig. 1. Temperature-programmed reduction analysis of Fe_3O_4.

At temperatures higher than 450 °C other reduction processes are observed by two main broad overlapped peaks (Fig. 1). These peaks are related to the reduction of Fe_3O_4 to FeO and Fe^0 according to the processes [29]:

$$Fe_3O_4 + H_2 \rightarrow 3FeO + H_2O \quad (3)$$

$$FeO + H_2 \rightarrow Fe^0 + H_2O \quad (4)$$

Based on this TPR analysis the preparation of the composites Fe^0/Fe_3O_4 was carried out by reduction of the magnetite at 300 °C, 400 °C and 500 °C varying the reduction time from 1 h up to 4 h. The composites obtained with 2 h reduction were analyzed by XRD (Fig. 2 and Table 1), magnetization measurements (Table 1) and Mössbauer spectroscopy (Fig. 3).

XRD analyses of the starting Fe_3O_4 showed the presence of the spinel phase with lattice parameter of $a_0 = 0.838$ nm. The broad XRD peaks, the smaller lattice parameter compared to pure magnetite ($a_0 = 0.8396$ nm) and the small magnetization of 63 J kg^{-1} T^{-1} (Table 1) suggests the presence of iron oxidized phases, e.g. the spinel maghemite. As the starting Fe_3O_4 is treated with H_2 at different temperatures a sharpening and gradual shift of the XRD peaks are observed (see detail, Fig. 2). At 300 °C no new crystalline phase was detected in the XRD but an increase in the lattice parameter to 0.839 nm and an increase in magnetization to 72 J kg^{-1} T^{-1} clearly show the reduction of the oxidized phases to form Fe_3O_4. Powder XRD
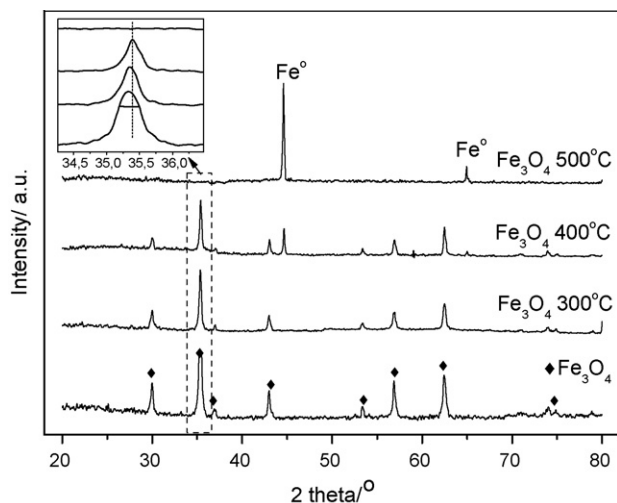
Table 1
XRD lattice parameters (a_0) and magnetization for the Fe_3O_4 reduced with H_2 at different temperatures for 2 h

Reduction temperature (°C)	a_0 (nm)	Magnetization (J kg^{-1} T^{-1})
Not reduced	0.838	63
300	0.839	72
400	0.839	92
500C	–	135

of the sample reduced at 400 °C revealed the formation of Fe^0 with crystallite size of *ca.* 85 nm as estimated by Scherrer's equation with an increase in the magnetization to 92 J kg^{-1} T^{-1}. Reduction at 500 °C resulted only the presence of Fe^0 metal crystalline phase with particle size of *ca.* 112 nm and a magnetization of 135 J kg^{-1} T^{-1}.

Similar results for the Fe_3O_4 reduced with H_2 have been obtained by Mössbauer spectroscopy.

The CEMS spectrum for the starting magnetite showed the presence of the spinel Fe_3O_4 (with hyperfine field 49.0 T for the octahedral site and 46.0 T for the tetrahedral site, and isomer shifts of 0.17 mm s^{-1} and 0.54 mm s^{-1}) with 85% relative signal intensity and 15% of maghemite, γ-Fe_2O_3 (Fig. 3 and Table 2). As maghemite, γ-Fe_2O_3, also has a spinel structure it cannot be easily differentiated from Fe_3O_4 by XRD. If this magnetite was treated with H_2 at 300 °C the CEMS showed that the γ-Fe_2O_3 was reduced to produce Fe_3O_4 (Table 2). Upon reduction at 400 °C and 500 °C a new Mössbauer signal with hyperfine field at 33 T related to Fe^0 can be clearly observed (Fig. 3 and Table 2).

Table 2 presents the Mössbauer parameters obtained for the starting Fe_3O_4 and reduced samples.
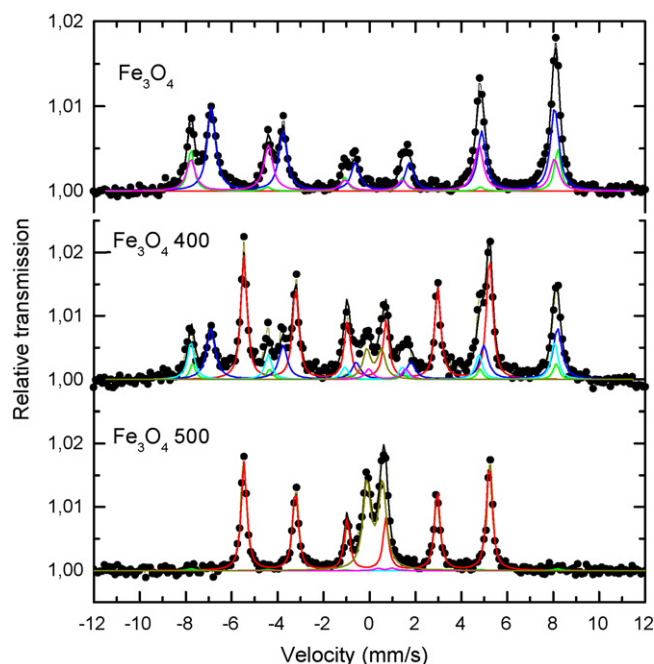

Fig. 2. Powder XRD for the magnetite before and after reduction with H_2 at 300 °C, 400 °C and 500 °C for 2 h.

Fig. 3. CEMS of the starting Fe_3O_4 and after reduction at 400 °C and 500 °C with H_2 for 2 h.

Table 2
Mössbauer parameters of Fe_3O_4 reduced with H_2 at different temperatures for 120 min and 240 min

Treatment	Phases	$\delta \pm 0.05$ (mm s^{-1})	$\Delta \pm 0.05$ (mm s^{-1})	$B_{hf} \pm$ (T)	Area $\pm$ 2 (%)
Starting Fe_3O_4	γ-Fe_2O_3	0.29	−0.01	49.5	15
	Fe_3O_4	0.57	0.02	46.4	55
		0.27	0.04	49.1	30
H_2, 300 °C per 2 h	Fe_3O_4	0.67	0.03	46.8	95
		0.25	−0.04	49.2	
	γ-Fe_2O_3	0.29	−0.01	49.5	5
H_2, 400 °C per 2 h	Fe^0	0	0.00	33	47
	γ-Fe_2O_3	0.33	−0.01	49.1	5
	Fe_3O_4	0.68	0.03	46.8	25
		0.27	−0.04	49.2	15
	Fe^{3+}	0.80	1.2	–	2
		0.30	0.63	–	6
H_2, 400 °C per 2 h (after 24 h exposition to air)	Fe^0	0	0.00	33	33
	γ-Fe_2O_3	0.33	−0.01	50.1	8
	Fe_3O_4	0.67	0.03	46.7	26
		0.25	−0.04	49.2	15
	Fe^{3+}	0.45	−0.74	–	10
		0,24	0.68	–	9
H_2, 500 °C per 2 h	Fe^0	0	0.00	33	66
	γ-Fe_2O_3	0.33	−0.01	49.5	–
	Fe_3O_4	0.67	0.03	46.8	–
		0.25	−0.04	49.2	–
	Fe^{3+}	0.33	−0.04	–	–
			0.68	–	34
H_2, 500 °C per 4 h	Fe^0	0	0.00	33	98
	Fe^{3+}	0.33	−0.04	–	2

Table 2 shows that the reduction at 400 °C for 2 h produced 47% Fe^0. On the other hand, large amounts of oxidized phases such as Fe_2O_3 and Fe^{3+} highly dispersed were formed after reduction at 500 °C for 2 h. The formation of these oxidized phases cannot be explained by the reaction with H_2 and is likely produced by oxidation upon exposure to air (Eq. (5)).

$$\text{Reactive } Fe^0 \text{ or } Fe_3O_4 + O_2(\text{air}) \rightarrow Fe^{3+} \text{ oxidized species} \quad (5)$$
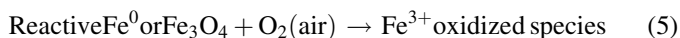
In fact, comparison of the CEMS of Fe_3O_4 immediately after reduction at 400 °C and after exposure to air at room temperature for 24 h clearly shows that Fe^0 is slowly oxidized decreasing from 47% to 33% with the concomitant increase of Fe^{3+} species from 5% to 19% (Fig. 4 and Table 2). These results suggest that the composites formed are fairly reactive towards O_2 even at room temperature. The composites were kept under N_2 to avoid slow oxidation by air before reactions with H_2O_2.

On the other hand, upon reduction at 500 °C for 4 h the Fe^0 was produced with 98% which suggests that a more stable Fe^0 metal phase was formed. Although the reason for this higher stability is not clear it might be related to sinterization/crystallization processes occurring during the 4-h treatment which produce Fe^0 particles more stable towards the oxidation by air.

If the transmission and conversion Mössbauer spectra of the composites are compared an important difference is observed.

The transmission Mössbauer spectrum shows the presence of a lower relative concentration of iron metal (32%) and higher

magnetite (64%) compared with the CEMS spectrum with Fe^0 47% and Fe_3O_4 25% (Fig. 5). As the CEMS technique provides information on the more superficial part of the composite (2500 Å), this result suggests that the composite has a higher Fe^0 concentration on the surface.

3.2. Peroxide decomposition

The composites obtained by the reduction of Fe_3O_4 with H_2 under different conditions were used to promote the hydrogen peroxide decomposition.

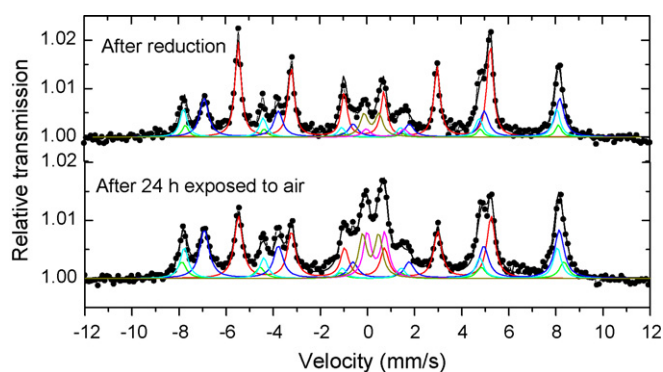$$H_2O_2 \xrightarrow{Fe_3O_4} H_2O + 0.5 O_2 \quad (6)$$

Fig. 4. Mössbauer immediately after reduction at 400 °C per 2 h and after 24 h exposed to air at room temperature.
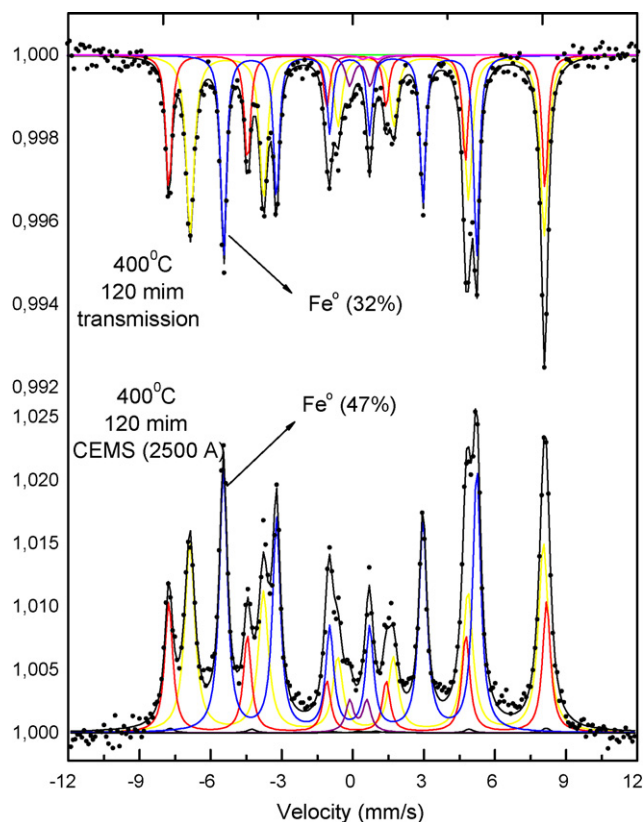
Fig. 5. The Mössbauer transmission and CEMS analyses for the magnetite reduced at 400 °C for 2 h.

Fig. 6. Peroxide decomposition in the presence of Fe_3O_4 reduced at different conditions ([H_2O_2] = 2.7 mol L^{-1}, pH 5.5 ± 0.2, composite 30 mg).

The hydrogen peroxide decomposition is a versatile probe reaction to investigate the activity of heterogeneous systems towards the Fenton chemistry. Although, this reaction is known to take place by a multi-step complex mechanism [31,32] a simplified reaction pathway can be considered for the decomposition in the presence of iron species, where the initial step is the reduction of H_2O_2 by Fe^{2+}:

$$Fe^{2+}_{magnetite} + H_2O_{2(aq)} \rightarrow Fe^{3+}_{magnetite} + HO^{\bullet} + HO^- \qquad (7)$$
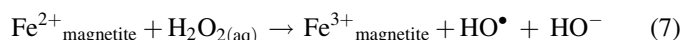
The $HO^{\bullet}$ radical can then react with another H_2O_2 molecule to produce the peroxide radical:

$$HO^{\bullet} + H_2O_{2(aq)} \rightarrow HOO^{\bullet} + H_2O \qquad (8)$$
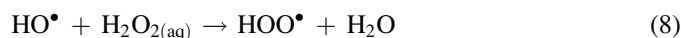
Finally, the hydroperoxide radical transfers one electron to $Fe^{3+}_{magnetite}$ species to produce the O_2 molecule:

$$HOO^{\bullet} + Fe^{3+}_{magnetite} \rightarrow Fe^{2+}_{magnetite} + H^+ + O_{2(g)} \qquad (9)$$
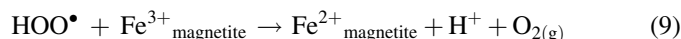
The obtained results for the peroxide decomposition in the presence of Fe^0/Fe_3O_4 produced by reduction with H_2 at different conditions are shown in Fig. 6.

It can be observed that the starting Fe_3O_4, commercial Fe^0 and their mechanical mixtures are nearly inactive for the decomposition of the H_2O_2. Upon reduction with H_2 at 300 °C, a significant increase on the activity was produced. This increase is likely related to the reduction of Fe^{3+} oxidized phases which are covering the surface of the Fe_3O_4 particles to produce active species $Fe^{2+}_{magnetite}$ species. This result clearly indicates t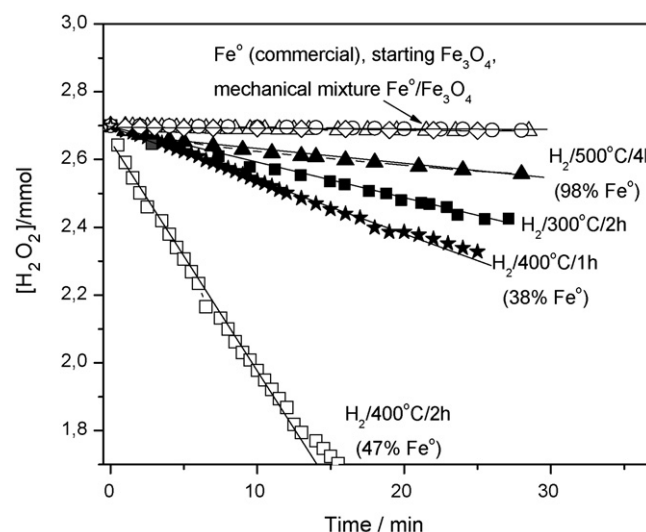hat $Fe^{2+}_{magnetite}$ species play an important role for the activation of H_2O_2. On the other hand, the reduction at 400 °C for 1 h and specially 2 h produced a remarkable increase on the decomposition activity. For these samples 38% and 47% of Fe^0, respectively, was formed, suggesting that the metal has a strong effect on the reactivity of the composites. It is interesting to note that the sample reduced at 500 °C for 4 h with 98% Fe^0 did not show a high activity. By the approximate linear behavior of the decomposition plots it can be approximated that the reaction has a pseudo zeroth order dependence on the H_2O_2 concentration. This is likely related to the high H_2O_2 concentration and similar kinetic behavior has been observed before [26–28]. The reaction rates can then be estimated by linear fit of the decomposition plots. The following rate constants for peroxide decomposition have been obtained: 0.41 mmol min^{-1} (for H_2/ 400 °C per 2 h) and 0.11 mmol min^{-1} (for H_2/500 °C per 4 h).

To investigate whether the Fe phases are reacting during the H_2O_2 decomposition, the composites were analyzed by CEMS before and after the peroxide decomposition (Fig. 7).

Table 3 presents the relative concentration of the different Fe phases, i.e. Fe_3O_4, Fe^0 and Fe^{3+}_{ox} (oxidized phases such as Fe_2O_3, FeOOH and Fe^{3+} highly dispersed) obtained by CEMS.

The starting oxidized Fe_3O_4 does not show any significant difference before and after the reaction with H_2O_2. On the other hand, the composite 400 °C/H_2 per hour after the reaction with H_2O_2 decreased the Fe^0 content from 38% to 35% with concomitant increase of the Fe^{3+} oxidized species. For the composite 400 °C/H_2 per 2 h the Fe^0 content decrease was even higher from 56% to 48%. These results clearly show that both Fe_3O_4 and Fe^0 are participating directly in the reactions with H_2O_2.

3.3. Oxidation of the dye methylene blue

The oxidation studies were carried out with the dye methylene blue and H_2O_2 as an oxidized agent. The dye methylene blue (MB) has several interesting features as a probe molecule for
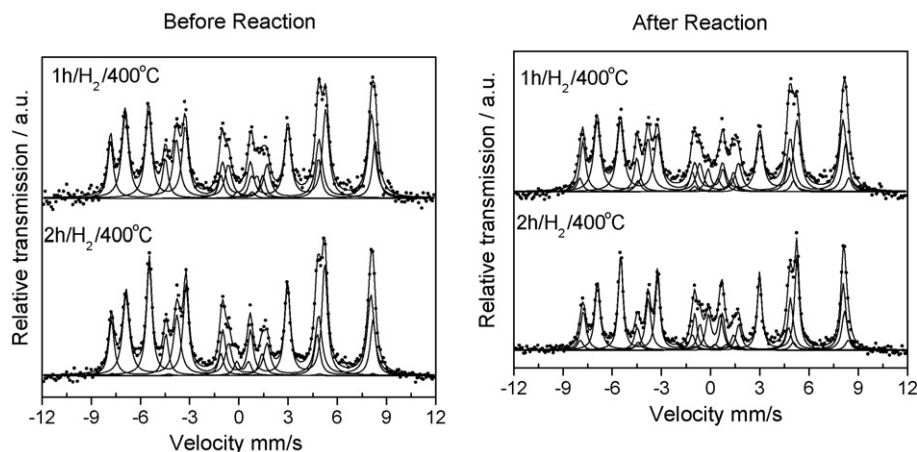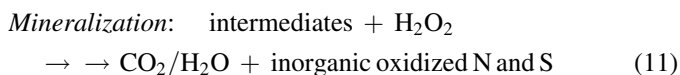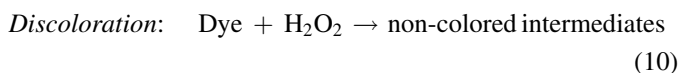
Fig. 7. Mössbauer spectra of the composites Fe^0/Fe_3O_4 (H_2/400 °C per hour or 2 h) before and after H_2O_2 reaction.

oxidation reactions, such as (i) MB shows high solubility in water, (ii) the oxidation of MB can be monitored by simple spectrophotometric measurements, (iii) due to the cationic nature of MB its adsorption on iron oxides (which have high PCZ [33]) strongly decreases, (iv) MB simulates the behavior of textile dyes which are an important class of contaminant and (v) MB is not easily reduced by pure iron metal [20].

The oxidation of the dye methylene blue was monitored by two parameters, i.e. the discoloration which is related to the first oxidation steps to produce non-colored intermediates and by total organic carbon related to the complete oxidation and mineralization of the organics to CO_2, H_2O and inorganic oxidized forms of N and S.

Discoloration: Dye $+ H_2O_2 \rightarrow$ non-colored intermediates
$$(10)$$

Mineralization: intermediates $+ H_2O_2$
$$\rightarrow \rightarrow CO_2/H_2O + \text{inorganic oxidized N and S} \qquad (11)$$

The discoloration activities of the composites obtained by reduction of Fe_3O_4 with H_2 at different conditions are shown in Fig. 8.

It can be observed that the starting Fe_3O_4 has a low activity with a discoloration of only ca. 10% after 120 min reaction. On the other hand, the Fe_3O_4 reduced at 300 °C presented a significant increase in the discoloration to 30% after 120 min reaction. These results suggest that Fe^{2+} species produced by the reduction at 300 °C play an important role on the discoloration

process. Upon reduction at 400 °C the discoloration activity strongly increased reaching almost 90% after 90 min reaction. It is interesting to note that the sample reduced at 500 °C for 4 h with 98% of Fe^0 and commercial Fe^0 did not present any significant activity for the discoloration of the dye methylene blue.

Although the kinetic in these reactions is very complex, a first-order dependence on the dye concentration could be adjusted (Fig. 9).

This is likely related to the relatively high initial concentration of H_2O_2 and the active catalyst which do not vary significantly in the beginning of the reaction. The pseudo first-order plot showed fairly linear behavior with rate constants of 0.001 min^{-1}, 0.004 min^{-1}, 0.020 min^{-1} and 0.027 min^{-1} for the Fe_3O_4 and the Fe_3O_4 reduced with H_2 at 300 °C, 400 °C per hour, 400 °C per 2 h, respectively (Fig. 9).

Analyses of the aqueous phase after the reaction by atomic absorption did not show any significant concentration of soluble iron. Also, several experiments revealed that the discoloration and H_2O_2 decomposition reactions immediately stop upon the removal of the catalyst from the medium by a simple magnetic
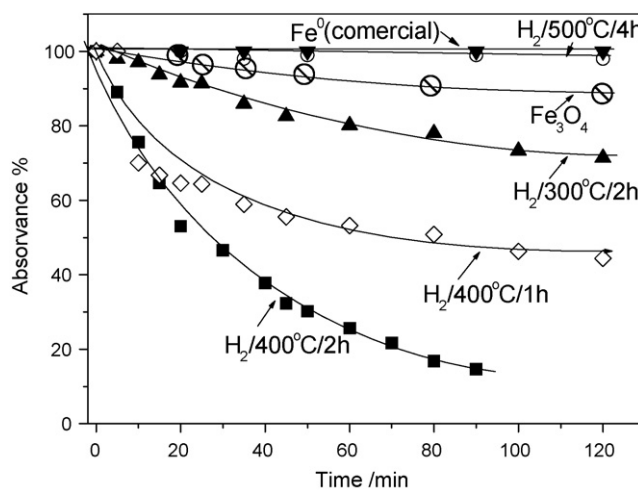
Table 3
Ratios $Fe_3O_4/Fe^0/Fe^{3+}_{ox}$ for the magnetite reduced at 400 °C determined by CEMS Mössbauer spectroscopy before and after the H_2O_2 decomposition reaction ([H_2O_2] = 2.7 mol L^{-1}, pH 5.5 ± 0.2, composite 30 mg)

Sample/treatment	$Fe_3O_4/Fe^0/Fe^{3+}_{ox}$ (ratio before reaction)	$Fe_3O_4/Fe^0/Fe^{3+}_{ox}$ (ratio after reaction)
Starting Fe_3O_4	79/0/21	79/0/21
H_2/400 °C per hour	53/38/9	53/35/12
H_2/400 °C per 2 h	56/41/3	48/38/14

Fe^{3+}_{ox}: oxidized iron (hematite, maghemite, goethite or highly dispersed amorphous Fe^{3+}).

Fig. 8. Discoloration of methylene blue (100 mg L^{-1}, 10 mL) in the presence of magnetite reduced with H_2 in different conditions ([H_2O_2] = 0.3 mol L^{-1}, pH 6.0 ± 0.2, catalyst 30 mg).
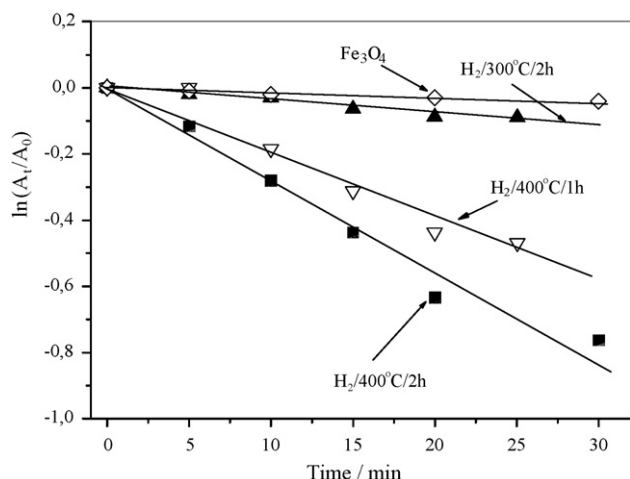
Fig. 9. Pseudo-first order kinetic plots for the discoloration of the dye methylene blue in the presence of Fe_3O_4 reduced at different conditions.

separation. These results clearly support a heterogeneous reaction initiated on the catalyst surface.

Total organic carbon was measured after 120 min reactions and the obtained results are shown in Fig. 10.

It can be observed that commercial Fe^0 did not produce a significant TOC reduction. The starting Fe_3O_4 produced a TOC reduction from *ca.* 60 mg L^{-1} to 45 mg L^{-1}. On the other hand, the Fe_3O_4 reduced with H_2 at 400 °C per 2 h showed 75% TOC reduction after 120 min reaction. It is interesting to compare with the Fe_3O_4 reduced with H_2 at 400 °C in the absence of H_2O_2 which showed only a small TOC reduction of *ca.* 10%. This TOC reduction in the absence of H_2O_2 is likely related to adsorption or some reduction process by Fe^0 or Fe^{2+} species. Discoloration and small TOC reduction have been reported previously for methylene blue in the presence of large amounts of Fe^0/Cu^0 mixtures [20].

3.4. Reaction mechanism

The results obtained in this work suggest that the reduction of Fe_3O_4 with H_2 to produce Fe^0/Fe_3O_4 composites has a strong
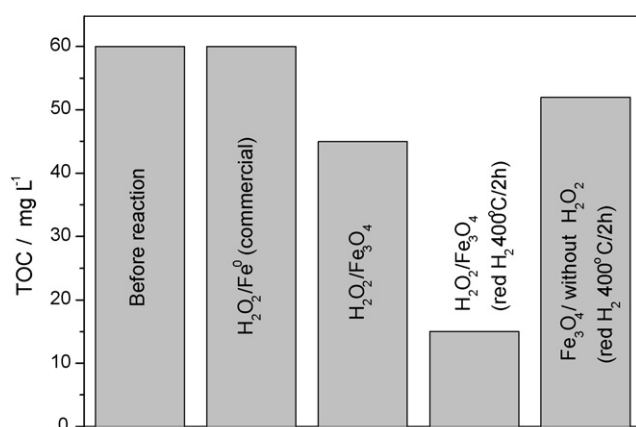

Fig. 10. Total organic carbon (TOC) after 120 min reaction of methylene blue (100 mg L^{-1}, 10 mL) in the presence of different systems ([H_2O_2] = 0.3 mol L^{-1}, pH 6.0 ± 0.2, composite 30 mg).

effect on the reactivity towards the H_2O_2 decomposition and the methylene blue oxidation. The rate constants for both reactions suggest that the reactivity of the system is favored by high Fe^0 content. However, the presence of Fe_3O_4 is also fundamental for a high activity since pure iron or 98% Fe^0 (composite 500 °C/H_2 per 4 h) is not active for the reactions.

It is interesting to observe that as the rate constant for H_2O_2 decomposition increases the discoloration rate also increases suggesting that both reactions are likely related in their mechanism.
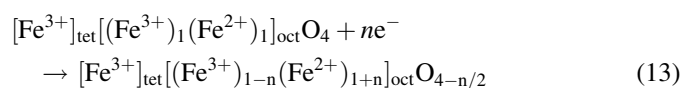
Previous work showed that the simple mixture of Fe^0 metal and Fe_3O_4 oxide by mechanical alloying also produces a significant increase in the activity for the Fenton reaction [26–28]. The reaction mechanism in these Fe^0/Fe_3O_4 alloyed mixtures has been discussed in terms of a facile electron transfer from Fe^0 to the reaction medium via the Fe_3O_4 to form $HO^{\bullet}$ radicals by the Haber–Weiss reaction (Eq. (12)).

$$Fe^0/Fe_3O_4 + H_2O_2 \rightarrow Fe^{3+}_{surf} + HO^{\bullet} + HO^{-} \tag{12}$$
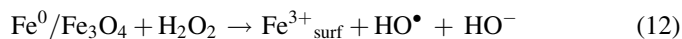
In fact, electrospray analyses of the reactions of phenol, aniline and chlorobenzene with H_2O_2 in the presence of Fe_3O_4 and mechanical mixtures of Fe^0/Fe_3O_4 have shown the formation of several hydroxylated intermediates, which strongly supports the participation of hydroxyl radicals in the reaction [27].

The formed hydroxyl radical can then react by two different and competitive pathways: (i) the oxidation of organics and (ii) the reaction with H_2O_2 leading to the decomposition to O_2 via $HOO^{\bullet}$.

It is interesting to consider two points about the reactivity of Fe^0: (i) Fe^0 commercial did not have any significant reactivity whereas Fe^0 in the composites was highly reactive towards H_2O_2 and even O_2 from the air as shown by the Mössbauer studies and (ii) Fe^0 commercial can become significantly more reactive by simply grinding with Fe_3O_4 as demonstrated before [26–28]. These results seem to suggest a special effect produced by the interaction of Fe^0 with Fe_3O_4. It can be speculated that Fe_3O_4 can aid the electron transfer from Fe^0 by acting as an intermediate/interface. In this mechanism the electron would be transferred initially from Fe^0 to $Fe^{3+}_{magnetite}$, to produce/regenerate $Fe^{2+}_{magnetite}$ which would be the active site for the reaction. Upon this interface reaction between Fe^0 and Fe_3O_4 a magnetite with higher concentration of Fe^{2+} at octahedral sites is formed according to the process shown in the following equation:

$$[Fe^{3+}]_{tet}[(Fe^{3+})_1(Fe^{2+})_1]_{oct}O_4 + ne^{-}$$
$$\rightarrow [Fe^{3+}]_{tet}[(Fe^{3+})_{1-n}(Fe^{2+})_{1+n}]_{oct}O_{4-n/2} \tag{13}$$

This electron transfer from Fe^0 to reduce Fe^{3+} species in the Fe_3O_4 phase is schematically represented in Fig. 11.

Some considerations to support this electron transfer are

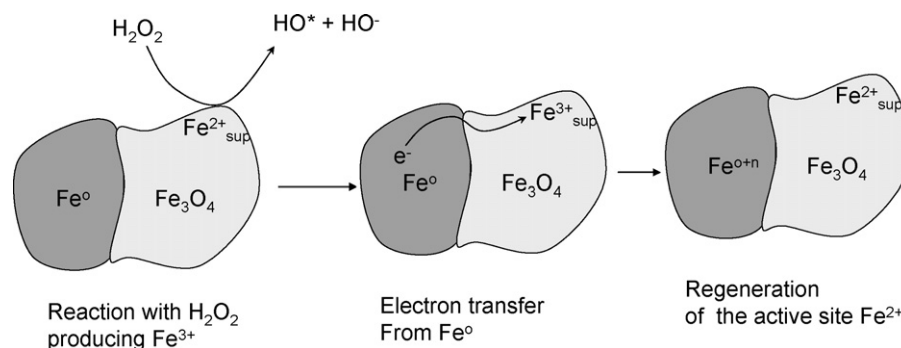(i) this process should be thermodynamically favorable as suggested by the standard equation:

$$Fe^0 + 2Fe^{3+} \rightarrow 3Fe^{2+}, \quad \Delta E^0 = 1.21 \text{ V} \tag{14}$$
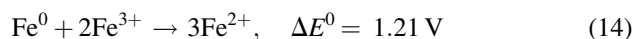
Fig. 11. Schematic representation of the electron transfer from Fe^0 to $Fe^{3+}_{magnetite}$ to regenerate Fe^{2+}_{surf}.

(ii) the octahedric site of the magnetite spinel structure is a very versatile redox site which can accommodate both Fe^{3+} and Fe^{2+}. Therefore, the Fe^{3+}_{oct} can be easily reduced to Fe^{2+}_{oct} with no structural constrain.

(iii) Fe^0 and Fe_3O_4 can form a very good interface. The efficient interface and electron transport between the metal (Fe^0) and the oxide has been clearly observed by Regan et al. [34]. In this work the authors using X-ray absorption spectroscopy demonstrated that at the interface metal–oxide, several layers of the metal are oxidized whereas several layers of the oxide are reduced.

(iv) magnetite is a high conductivity semiconductor with a narrow band gap (0.1 eV) with almost metallic character (*ca.* 10^2 to 10^3 Ω^{-1} cm^{-1}) [35,36] which is also important for electron transport.

Another point to be considered to discuss the high reactivity of the composites Fe^0/Fe_3O_4 is a physical effect related to the production of highly reactive small particles of Fe^0 and Fe_3O_4 upon reduction with H_2. The formation of these small particles at relatively low temperatures, i.e. 400 °C, likely takes place via the wüstite phase FeO (Eq. (15)).

$$Fe_3O_4 + H_2 \rightarrow 3FeO + H_2O \quad (15)$$

Wüstite is a metastable phase [37] and tends to disproportionate into α-Fe^0 and Fe_3O_4 (Eq. (16)) below its eutectoid temperature, 570 °C [38]. Depending on the conditions of its formation and decomposition, wüstite can produce highly dispersed nanoparticles of Fe^0 and Fe_3O_4 [39].

$$4FeO \rightarrow Fe_3O_4 + Fe^0 \quad (16)$$

Small particles of iron metal and magnetite [32] and Fe metal [33–35] are well known to present increased reactivity towards electron transfer reactions. Therefore, the high reactivity of the composites Fe^0/Fe_3O_4 can be related to the small particle size produced during reduction with H_2. However, both effects, i.e. the interface effect between Fe^0 and Fe_3O_4 to facilitate electrons transfer reaction medium and the particle size effect to improve reactivity must be further investigated.

4. Conclusion

The results obtained in this work showed that very high active heterogeneous Fenton systems based on composites Fe^0/Fe_3O_4 can be obtained by controlled reduction of Fe_3O_4 with H_2. The high reactivity of these composites has been discussed in terms of a participation of $Fe^{2+}_{magnetite}$ surface species which initiate the Fenton reaction by a Haber–Weiss mechanism. Fe metal has a very important role to produce an active system by transferring electrons to reduce Fe^{3+} species and regenerate the Fe^{2+} active species. These results open completely new perspectives for the production of active heterogeneous Fenton systems by a simple reduction with H_2 of different iron containing precursors, e.g. low cost materials such as iron ores and hazardous wastes such as the red mud.

These composites showed an improved reactivity of Fe^0 metal by an efficient electron transfer process which should also have important implications for the use of iron as an environmental remediation agent as a reductant. Preliminary work in our laboratory also showed high reactivity of these systems to reduce Cr(VI) species in an aqueous medium.

References

[1] K.H. Chan, W. Chu, Environ. Technol. 24 (2003) 703–710.
[2] A.R. Vitolins, B.R. Nelson, S.A. Underhill, L.M.H. Thomas, Soil Sediment Contam. 12 (2003) 139–150.
[3] A.T. Lamley, Q. Wang, D.A. Saltmiras, Pesticide Decontam. Detox. ACS Symp. Ser. 863 (2004) 55–83.
[4] A. Cuzzola, M. Bernini, P.A. Salvadori, Appl. Catal. B: Environ. 36 (2002) 231–237.
[5] H.H. Huang, M.C. Lu, J.N. Chen, Water Res. 35 (2001) 2291–2299.
[6] G. Centi, S. Perathoner, T. Torre, M.G. Verduna, Catal. Today 55 (2000) 61–69.
[7] W.P. Kwan e, B.M. Voelker, Environ. Sci. Technol. 37 (2003) 1150–1158.
[8] W.P. Kwan, B.M. Voelker, Environ. Sci. Technol. 36 (2002) 1467–1476.
[9] S. Chou, C. Huang, Chemosphere 38 (1999) 2719–2731.
[10] J. Feng, X. Hu, H.Y. Yue, Y. Zhu, G.Q. Lu, Water Res. 37 (2003) 3776–3784.

[11] S.R. Kunel, B. Neppolian, H. Choi, J.W. Yang, Soil Sediment Contam. 12 (2003) 101–117.

[12] R.J. Watts, M.D. Udell, S.H. Kong, Environ. Eng. Sci. 16 (1999) 93–103.

[13] G.C. Miller, B.W. Tyre, R.J. Watts, J. Environ. Qual. 20 (1991) 832–838.

[14] J.H. Choi, S.H. Kong, R.J. Watts, Chemosphere 37 (1998) 1473–1482.

[15] R.M. Lago, R.C.C. Costa, J.D. Fabris, J.D. Ardisson, C.N. Silva, R.R.V.A. Rios, L.C.A. Oliveira, M.F.F. Lelis, J. Hazard. Mater. 129 (2006) 171–178.

[16] R.M. Lago, R.C.C. Costa, J.D. Fabris, J.D. Ardisson, C.N. Silva, R.R.V.A. Rios, L.C.A. Oliveira, M.F.F. Lelis, Catal. Commun. 4 (2003) 525–529.

[17] F.I. Khan, T. Husain, R.J. Hejazi, Environ. Manage. 71 (2004) 95–122.

[18] L. Diels, J. Dries, L. Bastiaens, D. Springael, S.N. Agathod, Environ. Sci. Technol. 38 (2004) 2879–2884.

[19] P.G. Tratnyek, S. Mam, Water Res. 34 (2000) 1837–1845.

[20] J. Liu, L.M. Ma, Z.G. Ding, T.Y. Gao, R.F. Zhou, W.Y. Xu, Chemosphere 55 (2004) 1207–1212.

[21] G. Roy, P. de Donato, T. Gorner, O. Barres, Water Res. 37 (2003) 4954–4964.

[22] J. Park, T. Lee, H. Lim, Y. Lee, Chemosphere 53 (2003) 479–485.

[23] D. Vlassopoulos, C.B. Andrews, M. Rafferty, P.A. O'Day, N.A. Rivera, Abstr. Pap. Am. Chem. Soc. 226 (2003) U587.

[24] D.H. Bremner, A.E. Burgess, D. Houllemare, K.C.V. Namkung, Appl. Catal. B 63 (2006) 15–19.

[25] M. Arienzo, J. Chiarenzelli, R. Scrudato, Chemosphere 44 (2001) 1339–1346.

[26] F.C.C. Moura, M.H. Araújo, R.C.C. Costa, J.D. Fabris, J.D. Ardisson, W.A.A. Macedo, R.M. Lago, Chemosphere 60 (2005) 1118–1123.

[27] F.C.C. Moura, M.H. Araujo, I. Dalmázio, T.M.A. Alves, L.S. Santos, M.N. Eberlin, R. Augusti, R.M. Lago, Rapid Commun. Mass Spectrom. 20 (2006) 1859–1863.

[28] F.C.C. Moura, G.C. Oliveira, M.H. Araujo, J.D. Ardisson, W.A.A. Macedo, R.M. Lago, Chem. Lett. 34 (2005), CL-050577.

[29] R.M. Lago, L.C.A. Oliveira, J.D. Fabris, R.V.R.A. Rios, W.N. Mussel, Appl. Catal. A 259 (2004) 253–259.

[30] J.M.D. Coey, O. Cugat, J.D. Fabris, Rev. Fís. Aplicada Instrum. 7 (1992) 25.

[31] Y.N. Lee, R.M. Lago, J.L.G. Fierro, J. González, Appl. Catal. A 215 (2001) 245–256.

[32] F.C.C. Moura, M.H. Araujo, J.D. Ardisson, W.A.A. Macedo, A.S. Albuquerque, R.M. Lago, J. Braz. Chem. Soc. 18 (2007) 322–329.

[33] J.B. Rosenholm, M. Kosmulski, E. Maczka, E. Jartych, Adv. Colloid Interface Sci. 103 (2003) 57–76.

[34] T.J. Regan, H. Ohldag, C. Stamm, F. Nolting, J. Luning, J. Stohr, R.L. White, Phys. Rev. B 64 (2001) 214422.

[35] A.J. Bard, J.K. Leland, J. Phys. Chem. 91 (1987) 5076–5083.

[36] A.F. White, Rev. Miner. 23 (1990) 467–509.

[37] A.P. Janczyk, J.C. Grenier, B. Miczko, Solid State Ionics 117 (1999) 95–103.

[38] J. Ding, W.F. Miao, E. Pirault, R. Street, P.G. McCormick, J. Alloys Compd. 267 (1998) 199–204.

[39] D.A. Emel'yanov, K.G. Korolev, M.A. Mikhailenko, A.V. Knot'ko, N.N. Oleinikov, Y.D. Tret'yakov, V.V. Boldyrev, Inorg. Mater. 40 (2004) 632–635.